NREL
NATIONAL RENEWABLE ENERGY LABORATORY

A Novel Approach for Correlating Capacitance Data with Performance During Thin-Film Device Stress Studies

Preprint

R.L. Graham and D.S. Albin
National Renewable Energy Laboratory

L.A. Clark
Primestar Solar

Presented at the SPIE Optics + Photonics 2011
San Diego, California
August 21-25, 2011

Conference Paper
NREL/CP-5200-52392
August 2011

Contract No. DE-AC36-08GO28308

NOTICE

Available electronically at http://www.osti.gov/bridge

Available for a processing fee to U.S. Department of Energy
and its contractors, in paper, from:

U.S. Department of Energy
Office of Scientific and Technical Information

P.O. Box 62
Oak Ridge, TN 37831-0062
phone: 865.576.8401
fax: 865.576.5728
email: mailto:reports@adonis.osti.gov

Available for sale to the public, in paper, from:

U.S. Department of Commerce
National Technical Information Service
5285 Port Royal Road
Springfield, VA 22161
phone: 800.553.6847
fax: 703.605.6900
email: orders@ntis.fedworld.gov
online ordering: http://www.ntis.gov/help/ordermethods.aspx

Cover Photos: (left to right) PIX 16416, PIX 17423, PIX 16560, PIX 17613, PIX 17436, PIX 17721

Printed on paper containing at least 50% wastepaper, including 10% post consumer waste.

A Novel Approach for Correlating Capacitance Data with Performance during Thin-Film Device Stress Studies

Rebekah L. Graham*[a], Laura A. Clark [b], and David S. Albin[a]
[a]National Renewable Energy Laboratory, 1617 Cole Blvd., Golden, CO 80401
[b]Primestar Solar, 14401 West 66th Way, Unit B, Arvada, CO 80004
*Rebekah.graham@nrel.gov; phone 1 303 275-4531; fax 1 303 630-2045; www.nrel.gov

ABSTRACT

A new data mining algorithm was developed to identify the strongest correlations between capacitance data (measured between -1.5 *V* and +0.49 V) and first- and second-level performance metrics (efficiency [η%], open-circuit voltage [V_{OC}], short-circuit current density [J_{SC}], and fill-factor [*FF*]) during the stress testing of voltage-stabilized CdS/CdTe devices. When considering only correlations between first- and second-level metrics, 96.5% of the observed variation in η% was attributed to *FF*. The overall decrease in V_{OC} after 1,000 hours of open-circuit, light-soak stress at 60 °C was about -1.5%. The most consistent correlation identified by the algorithm in this particular experiment between *FF* and third-level metric capacitance data during stress testing was between *FF* and hysteresis in the apparent CdTe acceptor density (N_a) between reverse and forward voltages scans, as determined in forward voltage bias. Since the contribution of back-contact capacitance to total capacitance increases with increasing positive voltage, this result suggests that degradation in *FF* was associated with decreases in N_a hysteresis near the CdTe/back contact interface.

Keywords: chemometrics, CdTe solar cell, durability, reliability, efficiency, capacitance-voltage measurement, data mining, algorithm

1. INTRODUCTION

Understanding solar cell efficiency and reliability is crucial for advancing the field of photovoltaic research. Changes in efficiency can be investigated as a function of processing, measurement, and stress conditions. As efficiency changes during accelerated lifetime testing (ALT), various measurement techniques can be used to observe which other performance characteristics also change as a function of a particular stress condition. With the increasing scope of measurement capability and information storage, it is increasingly important to be able to quickly analyze large amounts of data and determine the significance of and interconnectedness between different types of measurements. The ultimate goal is to accurately associate changes in efficiency with the degradation mechanisms responsible for those changes.

The "bottom line" for the photovoltaic industry is to increase module power output (efficiency) and to limit power loss (improved reliability) at a competitive price. A previous investigation [1] used first- and second-level correlations between changes in η% and changes in V_{OC}, J_{SC}, and *FF* in order to ascertain the durability of a set of high-efficiency cells over a range of stress temperatures from 60-120 °C. Since solar cell η% is determined by

$$\eta\% = \frac{V_{OC} J_{SC} FF}{\phi_{inc}} \quad (1)$$

(where ϕ_{inc}, the incident power density, is typically normalized to a solar value of 100 mW/cm^2), a comparison of the linear correlation coefficients (R^2) of $\Delta\eta$% versus ΔV_{OC}, ΔJ_{SC}, and ΔFF during stress testing was performed as a function of stress temperature. This analysis is shown in Figure 1. As a reference, a linear fit of a perfectly correlated set of *y* and *x* has $R^2 = 1$, and a linear fit of a completely non-correlated set of *y* and *x* has $R^2 = 0$. The moderate correlation of $\Delta\eta$% with ΔJ_{SC}, seen at lower stress temperatures, was associated with reduced optical attenuation due to S out-diffusion from the CdS. The most important variable affecting $\Delta\eta$% over the entire temperature range, approaching perfect

correlation at 120 °C, was Δ*FF*. This figure clearly shows that understanding the loss in *FF* would be helpful in understanding the loss in *η%*.

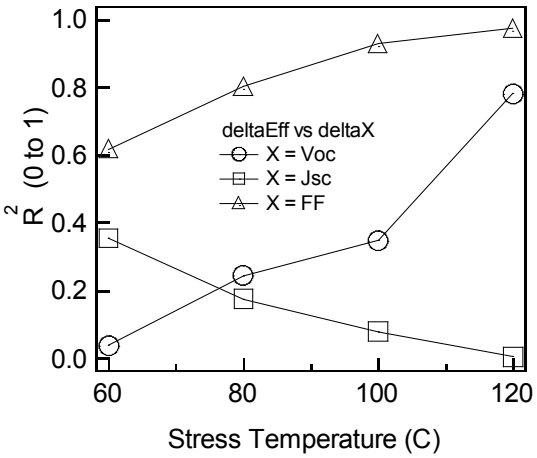

Figure 1. Linear correlation coefficient (R^2) of $\Delta\eta\%$ versus ΔV_{OC}, ΔJ_{SC}, and ΔFF, as a function of stress temperature (ref. [1]).

Arrhenius plots of overall efficiency change as a function of inverse temperature identified two dominant temperature-dependent degradation mechanisms. An activation energy for S diffusion into CdTe of 2.94 eV was determined for low stress temperatures (60-80 °C). At higher temperatures (100-120 °C), an activation energy for Cu diffusion into CdTe of 0.63 eV was determined to be responsible for the decreases in V_{OC} and *FF* observed at these temperatures.

The data mining technique described in this paper was developed to facilitate rapid identification of correlations between third-level metrics obtained with capacitance-voltage (*C-V*) measurements and first- ($\eta\%$) and second- (V_{OC}, J_{SC}, *FF,* light series resistance [R_S], and light and dark shunt resistance [$R_{SH,L}$ and $R_{SH,D}$]) level performance metrics. The technique is not limited to only *C-V* data and can be applied to other measurement techniques (e.g., photoluminescence, x-ray diffraction, deep-level transient spectroscopy, secondary ion mass spectrometry, etc.). This technique is optimally used for determining degradation mechanisms in a specific set of devices, preferably a set fabricated and stressed identically.

2. THE ALGORITHM

Chemometrics is a formal methodology applied to optimizing complex systems where many input variables contribute to one or more output parameters. The case for solar cells is obvious. Optimizing the performance, reliability, and cost of solar cells involves investigating many different materials (types of semiconductors, transparent conductors, metallic conductors, encapsulants, etc.), processes (evaporation, sputtering, close-spaced sublimation, etc.), and conditions of processing (temperatures, times, film thicknesses, deposition rates, etc.). The "design of experiment" approach using multivariate analysis is one chemometric approach for doing this efficiently. The latter was demonstrated, for example, in the fabrication of CdS/CdTe devices [2], where efficiency was optimized within the scope of input parameter variations associated with film thickness, $CdCl_2$ treatments, and back contact preparation. An important result of that study was that optimal performance did not result in optimal durability, the latter determined by stressing cells under one-sun illumination, open-circuit bias, and elevated temperature.

In the same way that correlations between first- and second-level metrics during stress testing are useful for broadly determining why cells degrade, similar correlations between second- and third-level metrics should be useful for more specifically identifying degradation mechanisms. *C-V* measurements have recently been used in cell stress studies [3-6] to qualitatively determine electronic changes in the device while performance changes with stress. To date, these studies have focused mostly on changes in the depletion width (W) and the apparent net acceptor density (N_a) as a function of stress. Advanced *C-V* analysis can also yield more intricate details associated with band offsets and interface states [7] as well as deconvolution of junction capacitance and back contact capacitance from total device capacitance [8].

Three important aspects we advocate when incorporating *C-V* measurements into stress studies include measuring capacitance as a function of voltage-sweep direction (reverse-to-positive bias [forward] versus positive-to-negative bias [reverse]), not exposing the cell to conditions too far removed from those the cell might encounter in actual module use (i.e., limit voltage), and the ability to collect data quickly in order to handle large sample sets for statistical purposes. The hysteretic behavior of *C-V* data (see for example [3]) is commonplace in CdTe (and in $CuInGaSe_2$ films, for that matter), can result in a bimodal distribution of *C-V*-derived parameters like W and N_a (something that device models should consider), and directly contributes to transient behavior in modules [9]. It is for this reason that our approach incorporates both forward- and reverse-direction voltage scans.

There are three levels of analysis in the data mining technique presented in this paper. These levels will be demonstrated within the context of a stress study, where measurements are made as a function of time during ongoing stress testing. In this example, the first- and second-level metrics and *C-V* are measured at several times during the stressing of a set of solar cell devices. The first level of analysis, shown in Figure 2(a), is to correlate $\eta\%$ with V_{OC}, J_{SC}, and FF, as a function of stress time. If $\eta\%$ is highly correlated with FF, as in this example, then looking for causes of FF degradation will illuminate possible causes of $\eta\%$ degradation and will suggest a road map for improved cell durability. The second level of analysis, shown in Figure 2(b), is to correlate FF with measurements of third-level metrics, such as capacitance, conductance (G), net acceptor density, and depletion width. Those *C-V*-derived data can be determined for each value of voltage in each voltage scan direction. This is performed for several identically processed devices, such that values of R^2 between that data and FF can be determined. In doing so, the voltage at which the highest correlation occurs (V_1) will be identified. The third level of this analysis technique, shown in Figure 2(c), is to choose the measurement condition of highest correlation and to look at the raw data, for example, FF versus W at $V = V_1$ as measured during the forward scan from negative to positive voltage bias.

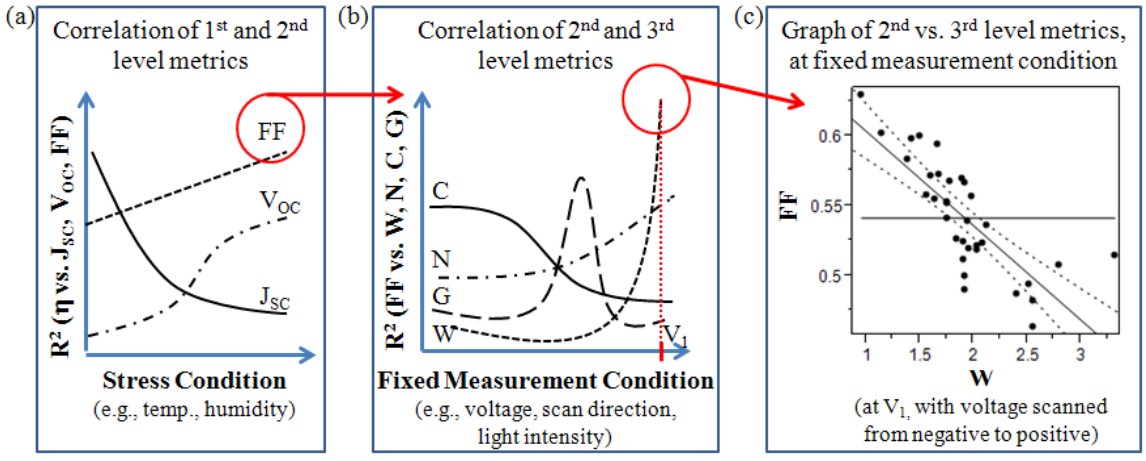

Figure 2. Outline of the (a) first, (b) second, and (c) third levels of the data mining technique presented in this paper. In order to understand power loss, this technique quickly reveals correlations between changes in the metrics that contribute to degradation of the output power.

The overall algorithm for this data mining technique is shown in Figure 3. For each device, light and dark current-voltage (*J-V*) scans yield values of η%, V_{OC}, J_{SC}, FF, R_S, $R_{SH,L}$, and $R_{SH,D}$. This data is stored in a database. The data mining code, currently written in but not limited to LabVIEW, then computes a *y*-versus-*x* linear fit at every fixed measurement condition, where $y = \eta$%, V_{OC}, J_{SC}, FF, R_S, $R_{SH,L}$, and $R_{SH,D}$, and x = the specified measurement at the fixed condition (e.g., $x = W$ at a specific voltage and in a specific direction of scanned voltage). Every linear fit produces a slope, intercept, and value of R^2.

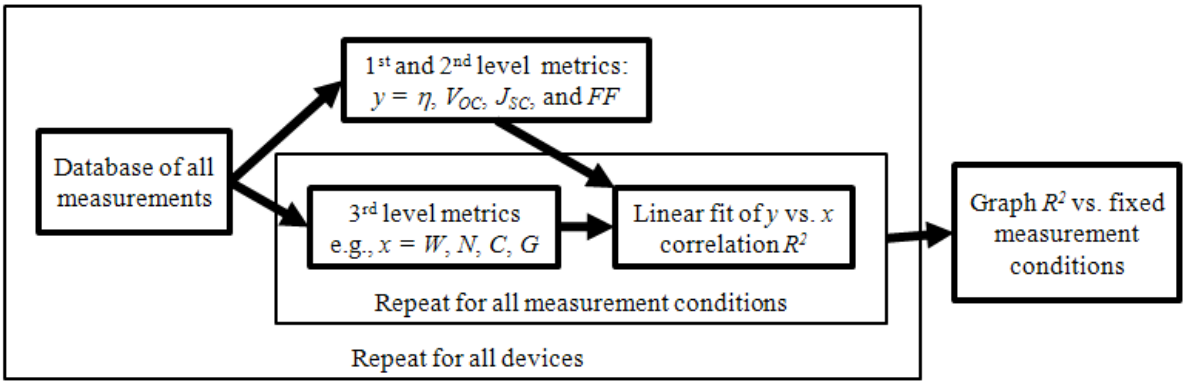

Figure 3. The data mining algorithm. The third-level metrics include any measurement data beyond the usual *J-V* measurement, with *C-V*-derived data shown as an example.

The linear fit, as opposed to any other type of fit, was chosen purely due to its predictive capabilities, i.e., we do not presume that a linear relationship exists. If two parameters are highly correlated, then it is possible to use the information from one of those parameters to predict the other parameter, without requiring both measurements. This correlation is especially valuable in stress studies, where it is useful to predict at what time a parameter will degrade beyond some specified value, which could indicate the predicted lifetime of the device.

3. RESULTS AND DISCUSSION

3.1 Algorithm Validation

This data mining approach will be demonstrated for a group of laboratory cells that show improved V_{OC} durability compared to what we have reported in the past. Figure 4 shows the variation in V_{OC}, measured as a function of stress time during elevated temperature, one-sun, open-circuit bias ALT for four representative groups. Cells in group A were stressed at 100 °C and are standard devices where the CdTe layer is relatively thick (9 to 10 μm). These devices show an overall decrease in V_{OC} of about 1.5% after 2,000 hours. Cells in group B were also stressed at 100 °C and were made by the same processing conditions, except that the CdTe thickness was considerably reduced (2 to 3.5 μm). With only nominal changes in cell fabrication procedure, the degradation of the thinner cells is significantly greater (>10% V_{OC} degradation after 270 hours of stress). The conclusion from Figure 4(a) is that thinner CdTe devices are clearly less stable than thicker devices. Figure 4(b) again compares thicker (9 to 10 μm) CdTe cells in group C with thinner (approximately 4 μm) cells in group D, where both groups were stressed at 60-65 °C. In this case, the thinner cells of group D do not show the typically large decrease in V_{OC} during ALT. V_{OC} degradation after 1,000 hours for groups C and D is similar, with a decrease of around 1.2 to 1.3%. Obtaining stable CdTe devices while reducing film thickness is important because the latter is a major driver for reducing CdTe module cost [10]. Further discussions in this paper will concentrate primarily on devices from group D.

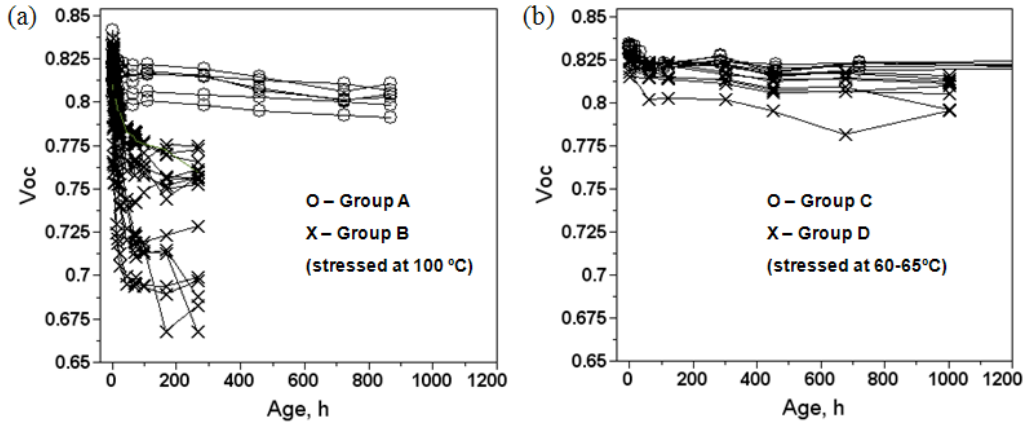

Figure 4. Degradation of V_{OC} for different processing variations during ALT at (a) 100 °C and (b) 60-65 °C.

A set of five CdS/CdTe devices in group D were stressed with 1,000 hours of ALT at 65 °C. In order to track performance changes during stress, these cells were characterized using *J-V* measurements at ALT times of 0 (unstressed), 60, 120, 300, 450, 675, and 1,000 hours. The *J-V*-derived parameters are shown as a function of stress age in Figure 5. R_S in Figure 5(e) was calculated from the inverse-slope of *J-V* at $J = 0$ mA/cm^2 under one-sun illumination. $R_{SH,L}$, and $R_{SH,D}$ in Figures 5(f) and 5(g) were calculated from the inverse-slope of *J-V* at $V = 0$ V with and without one-sun illumination, respectively. *C-V* measurements (at 100 kHz, with AC amplitude of 50 mV) were also performed in parallel with *J-V* measurements in order to validate the data mining algorithm.

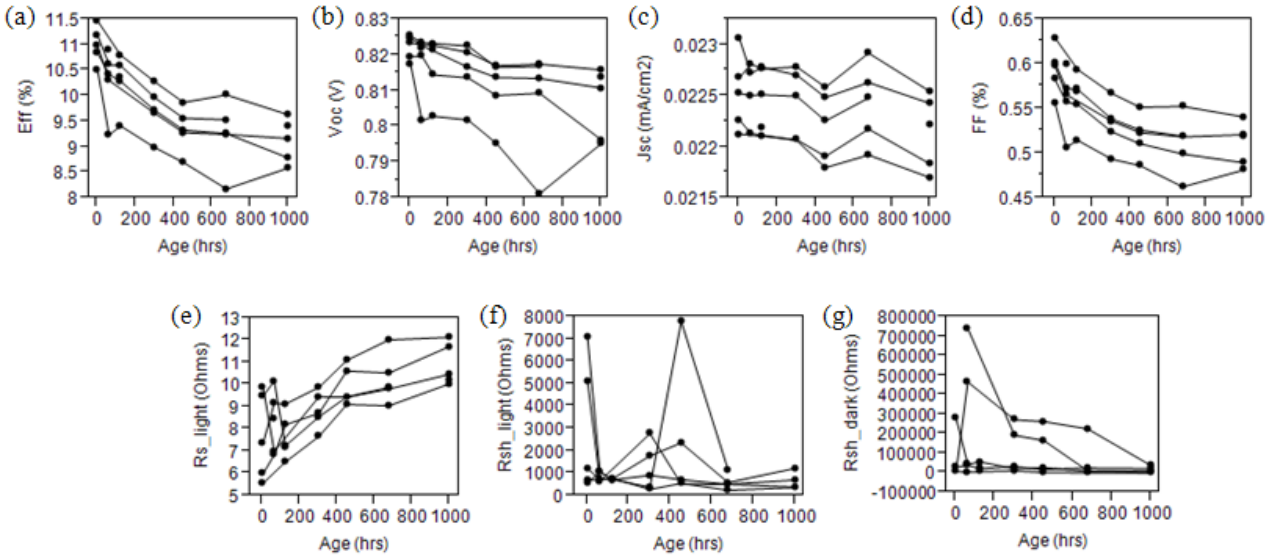

Figure 5. Graphs of (a) η%, (b) V_{OC}, (c) J_{SC}, (d) *FF*, (e) R_S, (f) $R_{SH,L}$, and (g) $R_{SH,D}$ versus age. Lines connect data collected from each of the five devices.

The first-level metric was plotted as a function of the second-level metrics, as shown in Figure 6. In Figure 6(c), η% has a 96.5% correlation with *FF* over the entire range of stress times, which indicates that 96.5% of the variation in η% can be explained by variations in *FF*. Furthermore, this means that if *FF* can be measured, then η% can be predicted with 96.5% accuracy. The relative stability of V_{OC} suggests that recombination is not a strong contributor to *FF* loss, thus *FF* loss was believed to be due primarily to degradation in either R_S or R_{SH}.

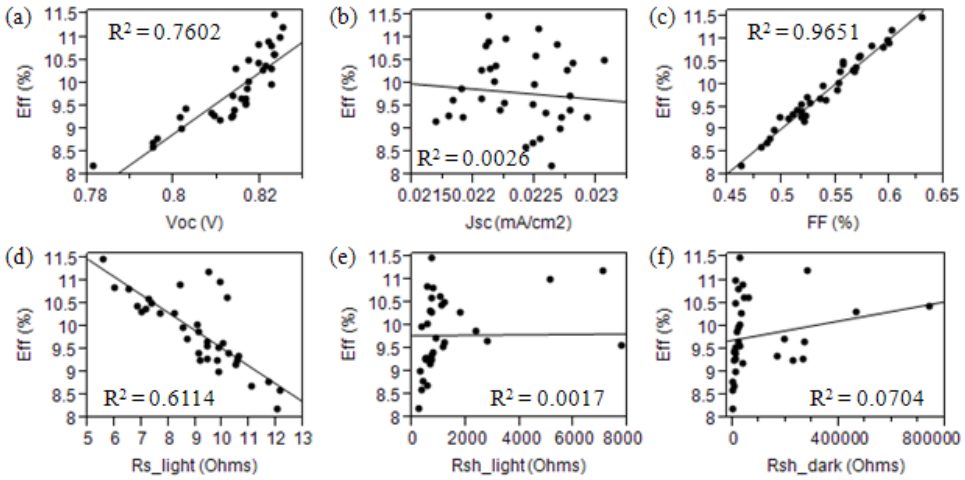

Figure 6. Graphs of $\eta\%$ versus (a) V_{OC}, (b) J_{SC}, (c) FF, (d) R_S, (e) $R_{SH,L}$, and (f) $R_{SH,D}$ for the aggregate of all five devices at all seven stress ages, shown with linear fits and corresponding values of R^2.

The power of the data mining algorithm will now be demonstrated as applied to C-V measurements. As mentioned previously, the algorithm determines all possible correlations between performance metrics ($\eta\%$, V_{OC}, J_{SC}, FF, R_S, $R_{SH,L}$, and $R_{SH,D}$) and a family of C-V-derived dependent variables for each set of different stress times, each voltage scan direction, and each incremental change of voltage. For illustration, Figure 7 shows a small subset of these correlations before stress ($t = 0$), between FF and C, G, W, and N_a, over the entire voltage range of the measurement, in both forward and reverse voltage scans. Also shown is the difference in C, G, W, and N_a determined between the two voltage scan directions (hysteresis, defined as the value measured in the forward scan minus the value measured in the reverse scan).

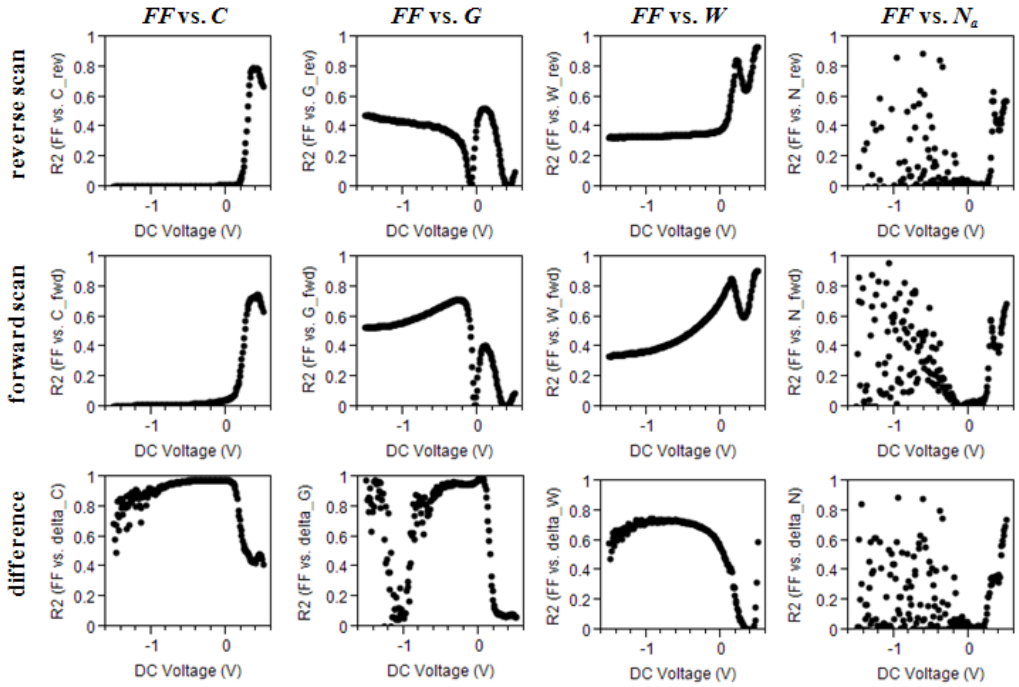

Figure 7. Correlation graphs showing R^2 at every voltage step for FF versus (columns, from left to right) C, G, W, and N_a as calculated from the (first row) reverse voltage scan, (second row) forward voltage scan, and (last row) difference between the measurements during the two scan directions, all for unstressed devices ($t = 0$).

Correlation graphs for y = η%, V_{OC}, J_{SC}, R_S, $R_{SH,L}$, and $R_{SH,D}$ are not shown. In Figure 7, it is easy to see that the correlation between first- and second-level metrics and third-level *C-V* metrics varies considerably with voltage but, in general, changes continuously. The data shown in Figure 7 is only for the set of *C-V* and performance data at t = 0, i.e., unstressed. The algorithm performs similar calculations at all stress times and, using a set of selection criteria and error checking routines to account for non-continuous behavior (like those shown for reverse bias in the *FF* versus N_a column in Figure 7), is able to identify the most consistent correlation during ALT studies useful for identifying degradation mechanisms.

Out of a possible set of 588 correlations, the algorithm identified two correlations as being the most consistent for this particular set of devices. These involved *FF* = *f*(N_a hysteresis*)* (shown for three arbitrary stress times in Figure 8) and η% = *f*(N_a hysteresis*)*, where N_a hysteresis was determined between the forward and reverse voltage sweeps at a voltage of +0.49 V. This result is in complete agreement with the first- and second-level correlation analysis shown in Figure 6. Since η% is so strongly correlated with FF, it is not surprising that the result of the algorithm included both *FF* and η%. The correlation with N_a hysteresis, however, is not a possible conclusion after only considering correlations between first- and second-level metrics.

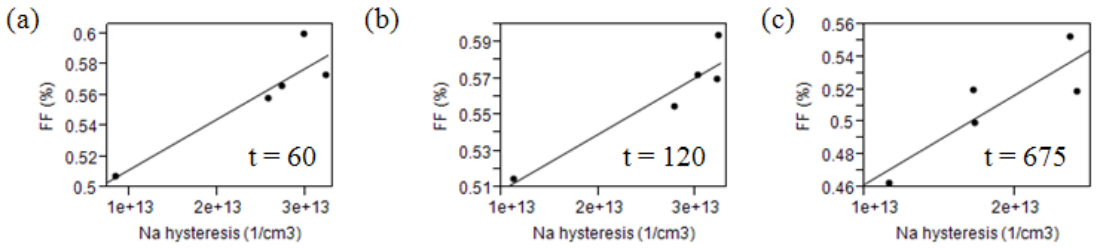

Figure 8. Graphs of *FF* versus N_a hysteresis at 0.49 V, as calculated between the forward and reverse voltage scans, after stress times of (a) 60 hours, (b) 120 hours, and (c) 675 hours.

The correlation between *FF* and N_a (in the forward and reverse scan directions and in the hysteresis between the two) at 0.49 V observed for all stress times is shown in Table 1. Since the correlation of FF = *f*(N_a hysteresis*)* shown in Figure 7 appears likely to increase with voltages higher than 0.49 V, we plan to use higher positive voltages in the future. The use of higher voltages during ALT, however, will require careful consideration of how higher forward currents during these measurements might compromise degradation. A likely explanation for why higher voltages yield better correlations in this particular experiment may be found in the literature. As shown in Figure 3 of the paper by Burgelman, et al. [8], in increasing the voltage beyond 0.49 V, the total cell capacitance is no longer determined by N_a hysteresis near the junction, but also by N_a hysteresis near the back contact. Based on this result, our data mining algorithm not only corroborates the information extracted from considering only first- and second-level metrics alone, but goes further in suggesting that cell degradation in this experiment is due to a decrease in N_a hysteresis near the interface between the CdTe and the back contact.

Stress Age	R^2 (*FF* vs. N_a, forward scan)	R^2 (*FF* vs. N_a, reverse scan)	R^2 (*FF* vs. N_a, hysteresis)
0	0.686	0.568	0.733
60	0.810	0.513	0.845
120	0.600	0.125	0.884
300	0.678	0.254	0.862
450	0.690	0.124	0.528
675	0.861	0.474	0.750
1000	0.408	0.001	0.698

Table 1. R^2 values for linear fits of *FF* versus N_a at 0.49 V, as calculated during the forward voltage scan, at each stress time.

4. CONCLUSIONS

A data mining approach was developed to efficiently analyze large amounts of data and to quickly identify correlations between first- and second-level performance metrics with third-level characterization data. It was applied specifically to *C-V* data collected during stress testing of laboratory cells, but should be applicable with other characterization techniques.

From a simple consideration of the correlation between cell efficiency and second-level metrics (V_{OC}, J_{SC}, FF), we determined that 96.5% of the variation in efficiency during stress for this set of devices could be explained by variations in FF. The data mining approach corroborated this result. With the algorithm, a large amount of data was reduced to only two correlations, both involving hysteresis in the apparent net acceptor density (N_a) measured at the maximum voltage used in our data collection (0.49 V) calculated from the difference in N_a between the forward and reverse voltage scans. With forward voltage bias, the measured capacitance sees contributions due to the reverse-biased back contact capacitance in addition to the forward-biased junction capacitance. The latter is also affected by injected charge (electrons) under forward bias, which is not considered in this paper. With this additional caveat, our results to date suggest that degradation in these cells is related to a decrease in N_a hysteresis at the CdTe/back contact interface.

5. ACKNOWLEDGEMENTS

This work was supported by the U.S. Department of Energy under Contract No. DE-AC36-08GO28308 with the National Renewable Energy Laboratory (NREL) and Primestar Solar through Cooperative Research and Development Agreement (CRADA) No. CRD-06-196 with Primestar Solar. The authors would also like to acknowledge discussions and assistance from Wyatt Metzger, Samuel Demtsu, Mark Pavol, Bogdan Lita, and Wes Dobson at Primestar Solar and James Johnson, Bastiaan Korevaar, and Oleg Sulima at the GE-Global Research Center during the duration of this work.

6. REFERENCES

[1] Albin, D., "Accelerated stress testing and diagnostic analysis of degradation in CdTe solar cells," Proc. SPIE 7048, 704825 (2008).
[2] Albin, D., Demtsu, S., McMahon, T., "Film thickness and chemical processing effects on the stability of cadmium telluride solar cells," Thin Solid Films 515, 2659-2668 (2006).
[3] Albin, D., Dhere, R., Glynn, S., del Cueto, J., Metzger, W., "Degradation and capacitance hysteresis in CdTe devices," Proc. SPIE 7412, 74120I (2009).
[4] Mendoza-Perez, R., Sastre-Hernandez, J., Contreras-Puente, G., Vigil-Galan, O., "CdTe solar cell degradation studies with the use of CdS as the window material," Solar Energy Materials & Solar Cells 93, 79-84 (2009).
[5] Demtsu, S., Albin, D., Pankow, J., Davies, A., "Stability study of CdS/CdTe solar cells made with Ag and Ni back-contacts," Solar Energy Materials & Solar Cells 90, 2934-2943 (2006).
[6] Corwine, C., Pudov, A., Gloeckler, M., Demtsu, S., Sites, J., "Copper inclusion and migration from the back contact in CdTe solar cells," Solar Energy Materials and Solar Cells 82, 481-489 (2004).
[7] Castillo-Alvarado, F.L., Inoue-Chavez, J.A., Vigil-Galan, O., Sanchez-Meza, E., Lopez-Chavez, E., Contreras-Puente, G., "C-V calculations in CdS/CdTe thin films solar cells," Thin Solid Films 581, 1796-1798 (2010).
[8] Burgelman, M., Nollet, P., Degrave, S., "Electronic behaviour of thin-film CdTe solar cells," Appl. Phys. A 69, 149-153 (1999).
[9] Del Cueto, J., Deline, C., Albin, D., Rummel, S., Anderberg, A., "Striving for a standard protocol for preconditioning or stabilization of polycrystalline thin film photovoltaic modules," Proc. SPIE 7412, 741204 (2009).
[10] Woodhouse, M., and Goodrich, A., private communication.